

First Precision Measurement of the Parity Violating Asymmetry in Cold Neutron Capture on ${}^3\text{He}$

M. T. Gericke^{1,*}, S. Baeßler,^{2,3} L. Barrón-Palos,⁴ N. Birge,⁵ J. D. Bowman,³ J. Calarco,⁶ V. Cianciolo,³ C. E. Coppola,⁵ C. B. Crawford,⁷ N. Fomin,⁵ I. Garishvili,⁵ G. L. Greene,^{5,3} G. M. Hale,⁸ J. Hamblen,⁹ C. Hayes,⁵ E. Iverson,³ M. L. Kabir,⁷ M. McCrea,^{1,10} E. Plemons,⁵ A. Ramírez-Morales,⁴ P. E. Mueller,³ I. Novikov,¹¹ S. Penttila,³ E. M. Scott,⁵ J. Watts,⁹ and C. Wickersham⁹

($n{}^3\text{He}$ Collaboration)

¹University of Manitoba, Winnipeg, Manitoba R3T 2N2, Canada

²University of Virginia, Charlottesville, Virginia 22904, USA

³Oak Ridge National Laboratory, Oak Ridge, Tennessee 37830, USA

⁴Universidad Nacional Autónoma de México, Mexico City, D.F., Mexico

⁵University of Tennessee, Knoxville, Tennessee 37996, USA

⁶University of New Hampshire, Durham, New Hampshire 03824, USA

⁷University of Kentucky, Lexington, Kentucky 40526, USA

⁸Los Alamos National Laboratory, Los Alamos, New Mexico 87545, USA

⁹University of Tennessee Chattanooga, Chattanooga, Tennessee 37403, USA

¹⁰University of Winnipeg, Winnipeg, Manitoba R3B 2E9, Canada

¹¹Western Kentucky University, Lexington, Kentucky 40526, USA



(Received 24 April 2020; accepted 4 August 2020; published 23 September 2020)

We report the first precision measurement of the parity-violating asymmetry in the direction of proton momentum with respect to the neutron spin, in the reaction ${}^3\text{He}(n, p){}^3\text{H}$, using the capture of polarized cold neutrons in an unpolarized active ${}^3\text{He}$ target. The asymmetry is a result of the weak interaction between nucleons, which remains one of the least well-understood aspects of electroweak theory. The measurement provides an important benchmark for modern effective field theory and potential model calculations. Measurements like this are necessary to determine the spin-isospin structure of the hadronic weak interaction. Our asymmetry result is $A_{\text{PV}} = [1.55 \pm 0.97(\text{stat}) \pm 0.24(\text{sys})] \times 10^{-8}$, which has the smallest uncertainty of any hadronic parity-violating asymmetry measurement so far.

DOI: 10.1103/PhysRevLett.125.131803

Introduction.—The electroweak component of the standard model (SM) describes the weak couplings of W and Z gauge bosons to quarks and therefore, in principle, the hadronic weak interaction (HWI). In nuclei, the HWI causes parity-violating (PV) admixtures in nuclear wave functions and produces small, but observable, PV spin-momentum correlations, photon circular polarizations, and anapole moments. However, the computational difficulties associated with nonperturbative QCD dynamics currently preclude first-principles calculations of hadronic PV observables. As a result, the HWI is the least well understood sector of the standard model. The most ambitious effort to carry out a QCD calculation on the lattice has been that of Wassem [1].

Desplanques, Donoghue, and Holstein (DDH) [2] introduced a physically motivated meson-exchange potential model. The resulting PV nucleon-nucleon potential is a sum over the six parity-odd, time-reversal-even, rotationally invariant operators that can be constructed from the

spin, isospin, momenta, and coordinates of the interacting nucleons and six meson-exchange coupling constants. The six floating coupling constants ($h_\pi^1, h_\rho^0, h_\rho^1, h_\rho^2, h_\omega^0$, and h_ω^1) are labeled by meson type and total isospin change (ΔI). Modern calculations recast this in terms of pionless effective field theory (EFT) and chiral EFT, using low energy constants [3–6]. To determine the spin-isospin structure of the HWI, one needs precision measurements of all PV asymmetries for which there are theoretical predictions, to constrain all couplings in the DDH theory or EFT.

An inherent problem in the experimental determination of the structure of the HWI is that asymmetries in calculable few-body systems are very small ($\sim 10^{-7} \rightarrow \sim 10^{-8}$) and difficult to measure. Here we present the first precision measurement of the parity-violating asymmetry in the direction of proton momentum with respect to the neutron spin, in the reaction ${}^3\text{He}(n, p){}^3\text{H}$, a few body system for which the asymmetry has been calculated, using both the

DDH framework and chiral EFT [3,4]. A previous null measurement of this observable is described in Ref. [7]. For a summary of previous measurements of PV asymmetries that constrain the HWI see Refs. [8–11].

Description of the experiment.—The $n^3\text{He}$ experiment ran at the Fundamental Neutron Physics Beamline (FnPB) [12], at Oak Ridge National Laboratory, at the Spallation Neutron Source (SNS), from December 2014 to December 2015. A brief overview of the $n^3\text{He}$ setup is given here. A detailed description of the experiment can be found in Refs. [13–17].

Intense 1 GeV proton pulses from the SNS accelerator are produced at a rate of 60 pulses/s. The protons interact with a mercury target producing neutrons of a few MeV, that are moderated in liquid hydrogen, at ≈ 20 K [12], to produce pulses of cold neutrons. The experiment was separated from the moderator by a supermirror neutron guide [12]. The pulsed nature of the beam, the neutron energy distribution at the moderator, and knowledge of the distance from the moderator to the detector (17.5 m) allowed accurate determination of the neutron energy at the detector using the neutron time of flight (TOF). To prevent slow neutrons from overlapping with faster neutrons in the following pulses the neutron energy range in each pulse was restricted to be between 2 meV and 9 meV, using a pair of TOF choppers [12]. The corresponding neutron fluence, after the polarizer, was 1.8×10^{10} n/s/MW [18]. The average delivered proton beam power varied from 0.7 to 1.4 MW.

The experimental setup is illustrated in Fig. 1. In the beam direction ($+\hat{z}$), starting at the exit of the neutron guide, the experiment consisted of a beam monitor, a supermirror neutron polarizer (SMP) [19], a resonant RF spin rotator (RFSR) [17,20], a holding field, and a target-detector ion chamber [13,14]. A set of magnetic field coils produced a 10 G homogeneous field to hold the neutron polarization from the polarizer to the target. The field

direction at the target was carefully aligned to the $+\hat{y}$ direction, the direction of neutron polarization after exiting the SMP. The thin, low absorption, beam monitor was used to monitor the relative neutron beam intensity and pulse shape to 10^{-4} fractional uncertainty for a single pulse.

The RFSR reversed the neutron polarization for every other pulse. The neutron beam was collimated to 8 cm in x (horizontal) by 10 cm in y (vertical). The neutrons captured in a combined target-detector wire chamber, filled with ^3He gas at a pressure of 0.43 atmospheres, at room temperature, absorbing the vast majority of neutrons in the selected energy range. The decay protons and tritons from the capture reaction ionized the ^3He gas, and the charges were collected on the chamber wires and amplified to voltage signals. The target was separated into 144 wire cell volumes, defined by the 144 signal wires and the four high voltage (HV) wires surrounding each [13,14]. Wires were oriented perpendicular to the beam direction, either in horizontal or vertical orientation, depending on the measurement mode (see below).

The energy of the final state proton and triton ($Q = 764$ keV) is large compared to the center of mass energy of the initial state so that recoil effects are negligible and the ^3H and p momenta are equal in magnitude and in opposite directions. Therefore, in the absence of parity violation, the cross section is spherically symmetric. Radiative capture on ^3He has a branching ratio of 10^{-8} [21] and is negligible. The experiment's primary measurement was the directional asymmetry in the emission direction of the proton (\hat{k}_p), with respect to the neutron spin (\hat{s}_n). The corresponding single event differential cross section is given by

$$\frac{d\sigma}{d\Omega} = \left(\frac{d\sigma}{d\Omega} \right)_c (1 + A_{\text{PV}} \cos \theta_y + A_{\text{PC}} \cos \theta_x). \quad (1)$$

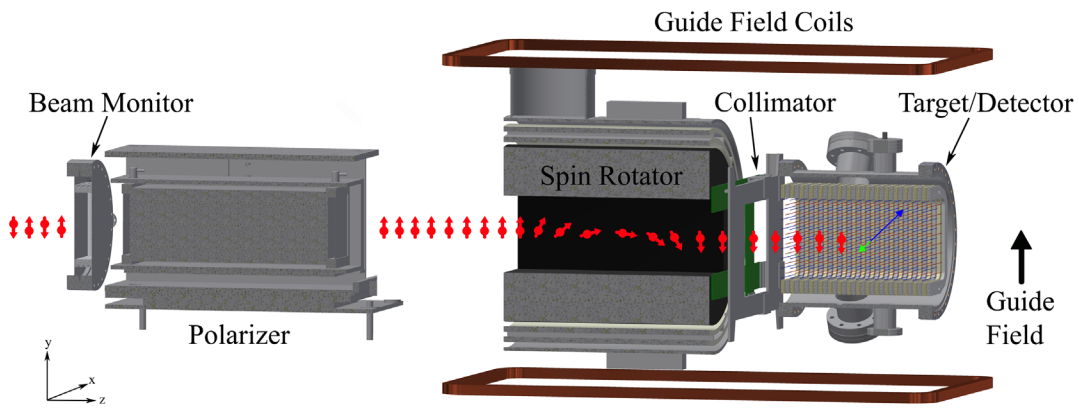


FIG. 1. Illustration of the $n^3\text{He}$ apparatus. Neutrons enter from the left and travel in the $+\hat{z}$ direction. The beam monitor measures the relative neutron beam intensity and pulse shape. Neutrons exit the supermirror with spins aligned upward (along $+\hat{y}$). The RF spin rotator reverses the spin direction every other beam pulse. Before entering the target the beam was collimated. Neutrons are captured in the target-detector chamber by ^3He , producing a proton and a triton per capture (the blue and green arrows, respectively).

Here, $(d\sigma/d\Omega)_c$ is the unpolarized capture cross section, A_{PV} is the parity-violating (PV) asymmetry and A_{PC} is the parity-conserving (PC) asymmetry. The PV asymmetry is a result of the correlation $\hat{s}_n \cdot \hat{k}_p = \cos \theta_y$, while the PC asymmetry is a result of the correlation $(\hat{s}_n \times \hat{k}_n) \cdot \hat{k}_p = \cos \theta_x$. For the definition of the PC correlation, we are generally using the coordinate system of Ohlsen and Keaton [22], but with the azimuthal angle ϕ measured from the spin axis y to the scattering normal, $\vec{n} = \hat{k}_n \times \hat{k}_p$. In spherical coordinates $\cos \theta_y = \sin \theta \sin \phi$ and $\cos \theta_x = \sin \theta \cos \phi$.

Referring to Fig. 1, since the average beam polarization is transverse, along $\pm \hat{y}$ (with the beam momentum equal to $k_n \hat{z}$), the vector $\hat{s}_n \times \hat{k}_n$ lies along the $\pm \hat{x}$ direction. Therefore, when the neutron spin is reversed the sign of the correlation terms flips along the corresponding axis. The PV asymmetry was extracted by measuring the signal with horizontal $[(\pm \hat{x})]$ wire orientation in the upper and lower hemispheres $(\pm \hat{y})$. This orientation rejects the PC (left-right) asymmetry and we refer to it as the up-down (UD) measurement mode. The PC asymmetry was measured by rotating the chamber 90 degrees around the beam axis, so that the wires were oriented vertically, rejecting the PV asymmetry. We refer to this orientation as the left-right (LR) measurement mode.

Data analysis.—Performing an energy deposition and wire cell acceptance weighted average of $\cos \theta_x$ and $\cos \theta_y$ in Eq. (1) yields an expression for the wire yields in terms of A_{PV} and A_{PC} , given by

$$Y_i^\pm = Y_i^0 [1 \pm \epsilon P (A_{\text{PV}} G_i^{\text{PV}} + A_{\text{PC}} G_i^{\text{PC}})] + p_i. \quad (2)$$

Here, the factors ϵ and P represent the polarization reversal efficiency and beam polarization, respectively. For the i th wire cell, Y_i^0 is the spin-independent signal yield, p_i is the signal pedestal, and G_i^{PV} , G_i^{PC} are the so-called geometry factors, replacing $\cos \theta_y$ and $\cos \theta_x$, respectively. Asymmetries for each wire were formed for each pair of opposite polarization states (indicated by \pm superscript)

$$A_i^{\text{meas}} = \frac{Y_i^+ - Y_i^-}{Y_i^+ + Y_i^-}. \quad (3)$$

In each spin state, data were taken for 15.68 ms, separated into 49 TOF bins. Since the neutron polarization is nearly flat in the energy range [20] and the PV asymmetry is independent of neutron energy, the signal in each spin state was summed over the TOF range.

Asymmetries were calculated either from single wire signals, according to Eq. (3), or for pairs of wires, for which the horizontal plane bisecting the chamber formed the mirror image (i.e., wire pairs with opposite sign but equal magnitude geometry factors). The wire pair asymmetries were formed in two ways:

$$A_i^{\text{meas}} = \frac{1}{2} \left(\frac{Y_{u,i}^+ - Y_{u,i}^-}{Y_{u,i}^+ + Y_{u,i}^-} - \frac{Y_{d,i}^+ - Y_{d,i}^-}{Y_{d,i}^+ + Y_{d,i}^-} \right), \quad (4)$$

and

$$A_i^{\text{meas}} = \frac{1}{2} \left(\frac{\frac{Y_{u,i}^+ - Y_{u,i}^-}{Y_{d,i}^+ - Y_{d,i}^-}}{\frac{Y_{u,i}^+ + Y_{u,i}^-}{Y_{d,i}^+ + Y_{d,i}^-}} \right). \quad (5)$$

Where u (up) and d (down) refer to wires the same distance above and below the chamber mirror plane, respectively. The method corresponding to Eq. (4) largely suppresses gain variations and any possible false asymmetry that couples to the gain, while method two [Eq. (5)] suppresses beam fluctuations and the associated beam asymmetry. The asymmetries calculated by all three methods were consistent with each other.

The measured asymmetries for each method were corrected for beam intensity asymmetries using linear regression with respect to the beam monitor data. The corresponding detector and monitor asymmetry slopes were below the few percent level. The accepted parity violating dataset consisted of 31 854, 7 min long runs. The analysis produced 128 single wire asymmetries or 64 wire pair asymmetries, which were then combined in a least-squares fit to extract the physics asymmetries (see below). Regression analysis of asymmetry versus random beam intensity fluctuations changed the central value by less than 0.04×10^{-8} .

The final analysis took into account all additive and multiplicative systematic effects (see Table I, the largest additive correction is associated with a twist in the wire frame stack (0 to 20 mrad front to back), which was carefully measured using survey equipment. The twist causes a correction, because it produces mixing between the LR and UD measurement modes, leading to the presence of PV and PC components in both sets of geometry factors.

To extract A_{PV} and A_{PC} , the data were analyzed by a least-squares fit of the measured wire pair asymmetries from the UD and LR mode datasets, to the coupled set of equations

$$\begin{aligned} A_{\text{UD},i}^{\text{meas}} &= \epsilon P (A_{\text{PV}} G_{\text{UD},i}^{\text{PV}} + A_{\text{PC}} G_{\text{UD},i}^{\text{PC}}) \\ A_{\text{LR},i}^{\text{meas}} &= \epsilon P (A_{\text{PV}} G_{\text{LR},i}^{\text{PV}} + A_{\text{PC}} G_{\text{LR},i}^{\text{PC}}), \end{aligned} \quad (6)$$

taking into account the wire correlation due to tracks crossing multiple cells. The correlations were obtained from measurement and verified with simulations. Neglecting the frame twist would remove the off-diagonal elements, $A_{\text{PC}} G_{\text{UD},i}^{\text{PC}}$ and $A_{\text{PV}} G_{\text{LR},i}^{\text{PV}}$, and produce the uncorrected asymmetries (neglecting systematic effects) $A_{\text{PV}}^{\text{uc}} = [1.22 \pm .91(\text{stat})] \times 10^{-8}$ and $A_{\text{PC}}^{\text{uc}} = [-41.0 \pm 5.6(\text{stat})] \times 10^{-8}$. A preliminary value for the expected size for A_{PC} is -35.0×10^{-8} [24,25].

TABLE I. Systematic corrections and errors.

Additive sources	Comment	Correction [ppb]	Uncertainty [ppb]
Frame twist (0 to 20 mrad)	Compare simulation and data [13]	2.5	0.2
Electronic false asymmetry A_{ped}	Measured [13]	0.0	2.0
Chamber field alignment	Compare simulation and data [13]	0.0	1.2
Geometry factors	Compare simulation and data [13]	0.0	0.5
Mott-Schwinger scattering	Published calculation [23]	-0.24	0
Residual ^3He polarization	Calculation [13]	< 0.001	0
Background (β, γ)	Simulation and calculation	$\ll 0.1$	0
In-flight β decay	Calculation [10]	$\ll 0.1$	0
Stern-Gerlach steering	Measurement and calculation (≤ 2 mG/cm)	$\ll 0.1$	0
Total		2.26	2.39
Multiplicative Sources			
Polarization	Measurement [15,20]	0.936	0.002
Spin-flip efficiency	Measurement [15,20]	0.998	0.001

The geometry factors and uncertainties ($G_{\text{UD},i}^{\text{PV}}$ and $G_{\text{UD},i}^{\text{PC}}$ for UD mode and $G_{\text{LR},i}^{\text{PC}}$ and $G_{\text{LR},i}^{\text{PV}}$ for LR mode) were determined by minimizing the difference between simulated and measured wire yields, while varying the simulated yield over many different chamber positions and gas fill pressures, within their respective measurement errors. The corresponding uncertainty in the asymmetry was determined by repeating the χ^2 minimization of Eqs. (6) for each simulated set of geometry factors. For the PV asymmetry, the result is shown in Fig. 2.

An overall rotation of the wire frame stack with respect to the holding field would also mix the PV and PC asymmetries. The rotation was carefully

measured to be zero, with an uncertainty of 3 mrad. The corresponding uncertainty in the PV asymmetry is $A_{\text{PC}} \times 3 \times 10^{-3} \simeq 0.12 \times 10^{-8}$. Equation (4) suppresses any forward backward asymmetry, that may be present due to residual longitudinal polarization. A possible false asymmetry from the RFSR signal coupling to the front-end detector and DAQ electronics was measured during weekly beam-off runs. The corresponding averaged beam-off or pedestal asymmetry is $A_{\text{ped}} = (0.024 \pm 0.2) \times 10^{-8}$. The ^3He target material produced extremely low background, being insensitive to gamma background. The signal background from neutron capture induced β decay in the target windows and other chamber materials was investigated using simulations and signal decay patterns in the chamber during beam-off periods; none were seen. Stern-Gerlach steering originates from the coupling of the neutron spin with a nonuniform gradient in the holding field (see Table I). The spin-orbit interaction between the neutron magnetic moment and the effective field of the target atom (Mott-Schwinger scattering [23]) produces a false left-right asymmetry, which is suppressed by the orientation and the wire pair combination in the asymmetry [Eqs. (4) and (5)]. Polarization of the target can arise due to the finite temperature ($P_{Th} \sim 2.3 \times 10^{-9}$), or from a gradual buildup, due to removal of selected ^3He spin states ($P_{Rm} \sim 6 \times 10^{-11}$), in the presence of a beam asymmetry. The resulting false asymmetries are at the 10^{-12} level. The beam polarization and spin-flip efficiency were measured in dedicated runs [15,20]. The final result, including statistical and all systematic errors is

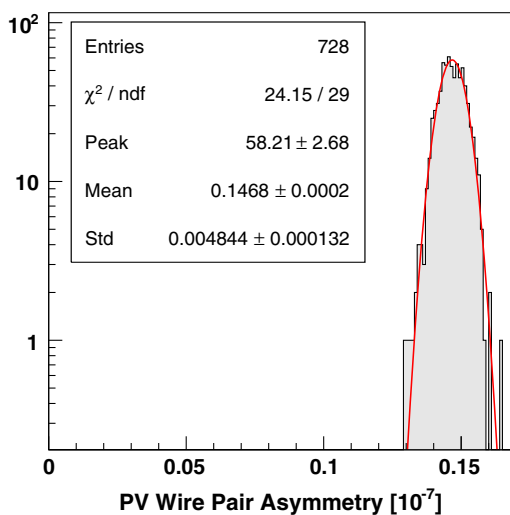


FIG. 2. Variation of PV wire pair asymmetries due to geometry factor uncertainty. The asymmetry was calculated 728 times (the vertical axis is the number of histogram entries), each with a different variation of the simulated geometry factors. The standard deviation sets the systematic error on the asymmetry due to uncertainty in the geometry factors (see text).

$$A_{\text{PV}} = [1.55 \pm 0.97(\text{stat}) \pm 0.24(\text{sys})] \times 10^{-8}. \quad (7)$$

Conclusion.—This result provides an important benchmark that extends our knowledge of the spin-isospin structure of the HWI, because the uncertainty in A_{PV} is

20 times smaller than the current theoretical reasonable ranges for the couplings, and the measurement was made in a few body system in which theoretical uncertainties are minimized. Viviani *et al.* calculated A_{PV} , using both, the DDH, and chiral EFT [3,4] framework. The first calculation uses the DDH potential for the weak interaction and a combination of the AV18/UIX potential [26–28] to describe the strong nucleon-nucleon interaction. In this framework, the asymmetry is given by [3]

$$A_{PV} = -0.185h_\pi^1 - 0.038h_\rho^0 - 0.023h_\omega^0 + 0.023h_\rho^1 + 0.050h_\omega^1 - 0.001h_\rho^2. \quad (8)$$

Using chiral EFT, including contact terms, and one- and two-pion exchange terms, they find [4]

$$A_{PV} = -0.137h_\pi^1 - 0.049h_\rho^0 - 0.023h_\omega^0 + 0.024h_\omega^1 + 0.015h_\rho^1 - 0.0001h_\rho^2. \quad (9)$$

Using the DDH [2] best values and ranges for the coupling constants the $n^3\text{He}$ asymmetry is predicted to be $A_{PV} = -0.6^{+8.3}_{-10.7} \times 10^{-8}$ and $A_{PV} = 2.1^{+13.3}_{-10.6} \times 10^{-8}$ for the two calculations, respectively. The coupling constants in Eqs. (8) and (9) are of order 10^{-7} .

More recently, Gardner *et al.* [29] calculate $A_{PV} \simeq -1.8 \times 10^{-8}$, based on the large- N_c framework [5,6] and the assumption that the $\Delta I = 1$ contribution to A_{PV} can be neglected. Our measured $n^3\text{He}$ asymmetry differs from the large- N_c prediction by 2.8σ .

The NPDGamma Collaboration measured $h_\pi^1 = (2.6 \pm 1.2) \times 10^{-7}$ [10]. Inserting this value into Eq. (8) gives a contribution to A_{PV} of -4.9×10^{-8} , indicating that there must be considerable cancellation between the h_π^1 term and heavy meson terms. When our result is combined with the NPDGamma measurement a constraint on a linear combination of heavy-meson couplings is obtained:

$$h_{\rho-\omega} \equiv h_\rho^0 + 0.605h_\omega^0 - 0.605h_\rho^1 - 1.316h_\omega^1 + 0.026h_\rho^2 = (-17.0 \pm 6.56) \times 10^{-7}. \quad (10)$$

These constraints are shown in Fig. 3. This analysis is possible because both reactions have been calculated with small model uncertainty, using the DDH potential model of the hadronic weak interaction [3]. A similar analysis in the chiral EFT framework would require a calculation of the NPDGamma asymmetry in that framework, which is underway [25].

Assuming the DDH values for the $\Delta I = 1$ and 2 couplings, we can estimate the size of the $\Delta I = 0$ terms, giving $h_\rho^0 + 0.61h_\omega^0 = (-18.6 \pm 6.6) \times 10^{-7}$. This supports the prediction of pionless EFT, that the $\Delta I = 0$ couplings may be large, and agrees with a previous, independent analysis, giving $h_\rho^0 + 0.7h_\omega^0 = (-25.9^{+6.1}_{-6.0}) \times 10^{-7}$ [9].

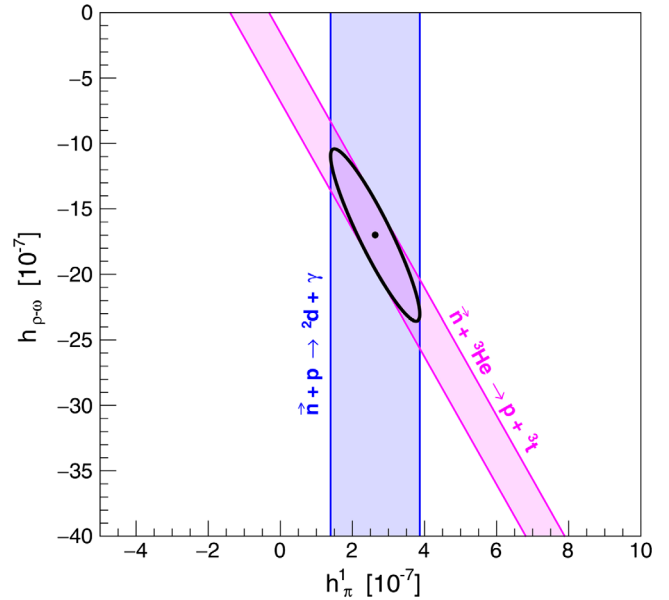


FIG. 3. A least squares fit to the NPDGamma [10] and the $n^3\text{He}$ asymmetry gives a constraint on a combination of heavy meson couplings, where $h_{\rho-\omega} \equiv h_\rho^0 + 0.605h_\omega^0 - 0.605h_\rho^1 - 1.316h_\omega^1 + 0.026h_\rho^2 = (-17.0 \pm 6.56) \times 10^{-7}$. See text for details.

In order to improve our knowledge of the spin-isospin structure of the hadronic weak interaction additional measurements in few-body systems with small experimental uncertainties are required. Equally important are calculations of the asymmetries with small model uncertainties. The $n^3\text{He}$ and NPDGamma experiments have increased the number of systems that meet these criteria from two to four.

We gratefully acknowledge the support of the U.S. Department of Energy Office of Nuclear Physics through Grants No. DE-FG02-03ER41258, No. DE-AC05-00OR22725, No. DE-SC0008107 and No. DE-SC0014622, the U.S. National Science Foundation Grant No. PHY-0855584, the Natural Sciences and Engineering Research Council of Canada (NSERC), the Canadian Foundation for Innovation (CFI), the Mexico National Council of Science and Technology (CONACYT) Grant No. 80444, and the UNAM research Grants (PAPIIT) No. IN111913 and No. IN109120. This research used resources of the Spallation Neutron Source of Oak Ridge National Laboratory, a DOE Office of Science User Facility. We also thank Michele Viviani (INFN Pisa) for very fruitful theory discussions and Jack Thomison (ORNL) for his engineering support.

*Michael.Gericke@umanitoba.ca

[1] J. Wasem, *Phys. Rev. C* **85**, 022501(R) (2012).
[2] B. Desplanques, J. F. Donoghue, and B. R. Holstein, *Ann. Phys. (N.Y.)* **124**, 449 (1980).

[3] M. Viviani, R. Schiavilla, L. Girlanda, A. Kievsky, and L. E. Marcucci, *Phys. Rev. C* **82**, 044001 (2010).

[4] M. Viviani, A. Baroni, L. Girlanda, A. Kievsky, L. E. Marcucci, and R. Schiavilla, *Phys. Rev. C* **89**, 064004 (2014).

[5] M. Schindler, R. P. Springer, and J. Vanasse, *Phys. Rev. C* **93**, 025502 (2016).

[6] D. R. Phillips, D. Samart, and C. Schat, *Phys. Rev. Lett.* **114**, 062301 (2015).

[7] V. A. Vesna *et al.*, *JETP Lett.* **33**, 20 (1981).

[8] B. Deplanques, *Phys. Rep.* **297**, 1 (1998).

[9] W. C. Haxton and B. R. Holstein, *Prog. Part. Nucl. Phys.* **71**, 185 (2013).

[10] D. Blyth *et al.*, *Phys. Rev. Lett.* **121**, 242002 (2018).

[11] H. E. Swanson, B. R. Heckel, C. D. Bass, T. D. Bass, J. M. Dawkins *et al.*, *Phys. Rev. C* **100**, 015204 (2019).

[12] N. Fomin, G. L. Greene, R. R. Allen, V. Cianciolo, C. Crawford, T. M. Tito, P. R. Huffman, E. B. Iverson, R. Mahurin, and W. M. Snow, *Nucl. Instrum. Methods Phys. Res., Sect. A* **773**, 45 (2015).

[13] M. McCrea *et al.*, arXiv:2004.10889.

[14] M. McCrea, Parity violation and cold neutron capture: A study of the detailed interaction between hadrons, Ph.D. Thesis, University of Manitoba, 2016.

[15] M. L. Kabir, A measurement of the parity violating asymmetry in the neutron capture on ${}^3\text{He}$ at SNS, Ph.D. thesis, University of Kentucky, 2017.

[16] C. E. Coppola, Measurement of parity violation in polarized neutron capture on ${}^3\text{He}$, Ph.D. Thesis, University of Tennessee, 2019.

[17] C. B. Hayes, Spin flipper, neutron polarimetry, and simulation, for the $n{}^3\text{He}$ experiment, Ph.D. thesis, University of Tennessee, 2016.

[18] E. Tang, An analysis of the parity violating asymmetry of polarized neutron capture in hydrogen from the NPDGamma experiment, Ph.D. thesis, University of Kentucky, 2015.

[19] S. Balascuta, R. Alarcon, S. Baeßler, G. Greene, A. Mietke, C. Crawford, R. Milburn, S. Penttila, J. Prince, and J. Schädler, *Nucl. Instrum. Methods Phys. Res., Sect. A* **671**, 137 (2012).

[20] M. M. Musgrave *et al.*, *Nucl. Instrum. Methods Phys. Res., Sect. A* **895**, 19 (2018).

[21] F. L. H. Wolfs, S. J. Freedman, J. E. Nelson, M. S. Dewey, and G. L. Greene, *Phys. Rev. Lett.* **63**, 2721 (1989).

[22] G. G. Ohlsen and P. W. Keaton, *Nucl. Instrum. Methods Phys. Res.* **109**, 41 (1973).

[23] M. T. Gericke, J. D. Bowman, and M. B. Johnson, *Phys. Rev. C* **78**, 044003 (2008).

[24] G. M. Hale (private communication).

[25] M. Viviani (private communication).

[26] R. B. Wiringa, V. G. J. Stoks, and R. Schiavilla, *Phys. Rev. C* **51**, 38 (1995).

[27] S. Veerasamy and W. N. Polyzou, *Phys. Rev. C* **84**, 034003 (2011).

[28] B. S. Pudliner, V. R. Pandharipande, J. Carlson, S. C. Pieper, and R. B. Wiringa, *Phys. Rev. C* **56**, 1720 (1997).

[29] S. Gardner, W. Haxton, and B. R. Holstein, *Annu. Rev. Nucl. Part. Sci.* **67**, 69 (2017).